Solid-State NMR Characterization of the Mineral Searlesite and Its Detection in Complex Synthesis Mixtures

Colin A. Fyfe,* Jørgen Skibsted,† and Wilhelm Schwieger‡

Department of Chemistry, University of British Columbia, Vancouver, British Columbia, Canada V6T 1Z1

Received May 8, 2001

The mineral searlesite ($NaBSi_2O_5(OH)_2$) was synthesized and characterized by ^1H, ^{11}B, ^{23}Na, and ^{29}Si magic-angle spinning (MAS) NMR spectroscopy. From these spectra, the ^{11}B and ^{23}Na quadrupole coupling parameters and isotropic chemical shifts and the ^{29}Si chemical shift anisotropies have been precisely determined. These parameters are all consistent with the local environments obtained from the crystal structure for searlesite from X-ray diffraction, and they demonstrate that the synthetic sample has a high degree of both short- and long-range order. Furthermore, these anisotropic parameters are found to provide a unique fingerprinting of searlesite in complex mixtures where the presence of this mineral is not anticipated. This is demonstrated for product mixtures formed in attempts to incorporate boron in the structures of the layer silicates magadiite and kenyaite. These mixtures have been investigated by ^{11}B, ^{23}Na, and ^{29}Si MAS NMR which clearly reveal that the samples are mixtures of searlesite and magadiite/kenyaite and that searlesite production consumes all of the boron in these synthesis mixtures. However, the ^{29}Si MAS NMR spectra of these mixtures indicate that the presence of boron in the reaction mixtures nevertheless has an important influence on the quality of the magadiite and kenyaite layer silicates produced.

Introduction

Various solid-state NMR techniques, particularly those involving magic-angle spinning (MAS) alone[1,2] or in combination with $\{^1H\}$-X cross polarization (CP),[3] have been developed for the characterization of solid materials and were applied with success as complements to diffraction experiments. For example, in addition to investigations of organic systems, considerable insight has been gained on the structures of such important inorganic materials such as gels, ceramics, catalysts, and minerals.[4] In general, the NMR data are sensitive to local ordering and structure in contrast to the long-range ordering and periodicities reflected in diffraction measurements.

In the present work, we report the application of a number of these techniques to the characterization of the mineral searlesite ($NaBSi_2O_5(OH)_2$) which has been synthesized for the first time, and we show that these techniques are diagnostic enough to unambiguously identify this compound in complex product mixtures. These mixtures represent attempts to incorporate boron in the structures of the layered silicates magadiite and kenyaite. These two minerals are materials which may potentially be used as catalysts and adsorbents if the charge densities of the layered compounds can be modified by direct isomorphous substitution of silicon by aluminum or boron during the synthesis process in a manner similar to that used for zeolites.[5−7] Furthermore, the interlayer sodium ions in these silicates are easily ion-exhanged which favors their use in detergent systems.[8] Most recently, magadiite has been used in the synthesis of composite mesoporous materials by the intercalation of various sources of silica and alumina between the magadiite layers.[9]

Searlesite ($NaBSi_2O_5(OH)_2$) is a natural borosilicate mineral whose crystal structure (monoclinic, $P2_1$) has been solved by single-crystal X-ray diffraction techniques.[10,11] The structure (Figure 1) contains two distinct SiO_4 tetrahedra in a framework, where each is connected to three SiO_4 units and one $BO_2(OH)_2$ tetrahedron. These tetrahedra form sheets running parallel to the (100) plane, and these sheets are held together by edge-sharing $NaO_2(OH)_4$ octahedra.

The crystal structures of magadiite and kenyaite with the idealized formulas $Na_2Si_{14}O_{29}\cdot xH_2O$ ($x = 8-10$) and $Na_2Si_{20}O_{41}\cdot 10H_2O$, respectively, remain unknown, probably because the crystals of both the natural and synthetic samples of these minerals are of colloidal size or contain large quantities of disordered atoms.[12] However, magadiite and kenyaite have

* To whom correspondence should be addressed. E-mail: fyfe@chem.ubc.ca. Fax: 604-822-2847.

† Present address: Instrument Centre for Solid-State NMR Spectroscopy, Department of Chemistry, University of Aarhus, DK-8000 Aarhus C, Denmark.

‡ Present address: Department of Technical Chemistry I, University of Erlangen-Nuremberg Egerlandstrasse 3, 91058 Erlangen, Germany.

(1) Andrew, E. R.; Bradbury, A.; Eades, R. G. *Nature* **1958**, *182*, 1659.
(2) Lowe, I. J. *Phys. Rev. Lett.* **1959**, *2*, 285.
(3) Schaefer, J.; Stejskal, E. O. *J. Am. Chem. Soc.* **1976**, *98*, 1031.
(4) *Solid-State NMR Spectroscopy of Inorganic Materials*; Fitzgerald, J. J., Ed.; ACS Symposium Series 717; American Chemical Society: Washington, DC, 1999.
(5) Bergk, K.-H.; Schwieger, W.; Porch, M. *Chem. Tech.* **1987**, *39*, 459; 508.
(6) Schwieger, W.; Brunner, E. *Colloid Polym. Sci.* **1992**, *270*, 935.
(7) Schwieger, W.; Pohl, K.; Brenn, U.; Fyfe, C. A.; Grondey, H.; Fu, G.; Kokotailo, G. T. *Stud. Surf. Sci. Catal.* **1995**, *94*, 47.
(8) Rojo, J. M.; Ruiz-Hitzky, E.; Sanz, J. *Inorg. Chem.* **1988**, *27*, 2785.
(9) Fudala, A.; Konya, Z.; Kiyozumi, Y.; Niwa, S.-I.; Toba, M.; Mizukami, F.; Lentz, P. B.; Nagy, J.; Kiricsi, I. *Microporous Mesoporous Mater.* **2000**, *35−36*, 631.
(10) Kravchenko, V. B. *Sov. Phys. Crystallogr.* **1964**, *9*, 143.
(11) Ghose, S.; Wan, C. *Am. Mineral.* **1976**, *61*, 123.
(12) Scholzen, G.; Beneke, K.; Lagaly, G. *Z. Anorg. Allg. Chem.* **1991**, *597*, 183.

10.1021/ic010487s CCC: $20.00
Published on Web 10/10/2001

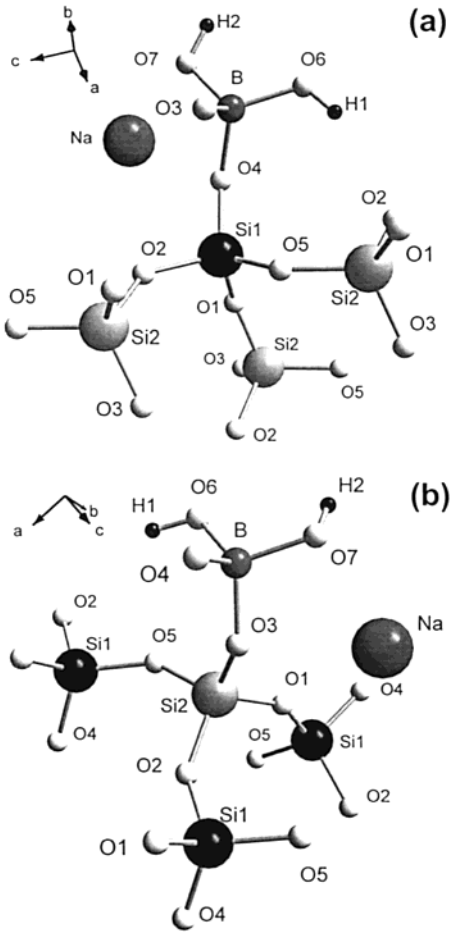

Figure 1. Perspective representation of the framework structure for (a) Si(1) and (b) Si(2) in searlesite ($NaBSi_2O_5(OH)_2$) based on the data from the reported single-crystal X-ray diffraction structure.[11]

been the subject to a number of ^{29}Si MAS NMR studies[14−20] which demonstrated that the basic layer structures of these minerals are made up of $HOSi^*(OSi)_3$, $NaOSi^*(OSi)_3$, and $Si^*(OSi)_4$ tetrahedra with sodium ions and H_2O molecules between these layers. Furthermore, recent ^{23}Na MAS and multiple-quantum MAS NMR studies have shown that magadiite and kenyaite both have a unique sodium site corresponding to sodium in octahedral coordination with relatively high symmetry.[21,22] However, it has not been possible to establish the connectivities of the individual SiO_4 tetrahedra in the layers of magadiite and kenyaite from which to construct the layer structures, presumably because the colloidal sizes of the crystals result in additional line broadening of the ^{29}Si NMR signals. The ^{29}Si MAS NMR spectra presented in this work for magadiite and kenyaite show that these phases are present in much more highly ordered forms when they are synthesized in boron-containing media.

Experimental Section

Materials. All reagents were from commercial sources; colloidal silica (30% SiO_2, 0.34% Na_2O) was from Chemiewerk, Bad Köstritz, and boric acid (solid) and NaOH pellets (≥97%) were both from Aldrich. Distilled water was used for the reaction mixtures which were made up by the dropwise addition over a period of 15 min of the silicate solutions (and boric acid if needed) to the stirred hydroxide solution. After the addition of all of the compounds was finished, the synthesis mixtures were further stirred vigorously for 30 min to set a homogeneous mixture. The mixtures were then heated at elevated temperatures in a 50-mL capacity rotating steel autoclave. The products were isolated by filtration and were washed thoroughly with distilled water. The molar oxide compositions of the mixtures, reaction temperatures, and crystallization times of the different syntheses were as follows: searlesite, 5.0 SiO_2:Na_2O:3.0 B_2O_3:72.2 H_2O, 150 °C, 336 h; "boron magadiite", 5.0 SiO_2:Na_2O:B_2O_3:72.2 H_2O, 125 °C, 552 h; "boron kenyaite", 5.0 SiO_2:Na_2O:B_2O_3:72.2 H_2O, 150 °C, 72 h; magadiite, 5.0 SiO_2:Na_2O:75 H_2O (note that no B_2O_3 was used in this synthesis), 150 °C, 136 h. The synthesis of the boron-free magadiite used a water glass (27% SiO_2, 8.8% Na_2O) as the silicon source. The X-ray powder diffraction patterns were obtained on a Rigaku Rotaflex diffractometer equipped with a copper (Cu Kα, $\lambda = 1.54184$ Å) rotating anode source.

NMR Measurements. The solid-state ^{1}H, ^{11}B, ^{23}Na, and ^{29}Si MAS NMR experiments were performed at 9.4 T on Bruker MSL-400 and DSX-400 spectrometers using triple-tuned 4- and 7-mm Bruker MAS probes or a home-built, double-tuned (X−Y) 14-mm MAS NMR probe equipped with a standard 14-mm stator from Chemagnetics. The single-pulse ^{1}H, ^{11}B, and ^{23}Na MAS experiments (4-mm probe) employed short rf excitation pulses (pulse widths of 0.5 μs (^{11}B), 1.0 μs (^{23}Na), and 2.0 μs (^{1}H)) for rf field strengths of $\gamma B_1/2\pi = 80$ kHz (^{11}B and ^{23}Na) and $\gamma B_1/2\pi = 100$ kHz (^{1}H). The {^{1}H}^{29}Si CP/MAS NMR spectra (7-mm probe) were recorded using rf field strengths of $\gamma B_1/2\pi = 50$ kHz and $\gamma B_2/2\pi = 60$ kHz for ^{29}Si and ^{1}H, respectively, while the single-pulse ^{29}Si MAS NMR spectra were obtained using the 14-mm MAS probe ($\gamma B_1/2\pi = 20$ kHz). Isotropic chemical shifts for ^{1}H and ^{29}Si are reported relative to tetramethyl siliane (TMS), while $\delta_{iso}(^{23}Na)$ and $\delta_{iso}(^{11}B)$ are relative to an aqueous 1.0 M solution of NaCl and a solid sample of $NaBH_4$, respectively. The simulations of the experimental NMR spectra were performed using programs described elsewhere,[23,24] and the error limits for the anisotropic NMR data were calculated using the procedure described in ref 25.

Results and Discussion

Searlesite. The presence of hydroxyl groups in near proximity to the silicon atoms in searlesite means that the ^{29}Si NMR resonances are most conveniently observed using {^{1}H}^{29}Si cross-polarization (CP) MAS NMR. Such spectra recorded at spinnings speeds of 3000 and 700 Hz are shown in Figure 2a and c, respectively, and clearly show two ^{29}Si resonances corresponding to the two inequivalent silicon sites. Furthermore, the spinning sideband (ssb) manifolds, observed at a low spinning speed, indicate large chemical shift anisotropies for both sites. Least-squares optimization of simulated to experimental ssb intensities for these overlapping manifolds yields the chemical shift anisotropy (CSA) parameters (δ_σ, η_σ, and δ_{iso}) listed in Table 1, and the goodness of the fit is illustrated by the simulated spectra in Figure 2b and d. The large shift anisotropies (δ_σ) for

(13) Schwieger, W.; Heidemann, D.; Bergk, K.-H. *Rev. Chim. Miner.* **1985**, *22*, 639.
(14) Pinnavaia, T. J.; Johnson, I. D.; Lipsicas, M. *J. Solid State Chem.* **1986**, *63*, 118.
(15) Rojo, J. M.; Sanz, J.; Ruiz-Hitzky, E.; Serratosa, J. M. *Z. Anorg. Allg. Chem.* **1986**, *540/541*, 227.
(16) Brandt, A.; Schwieger, W.; Bergk, K.-H. *Rev. Chim. Miner.* **1987**, *24*, 564.
(17) Heidemann, D.; Schwieger, W.; Bergk, K.-H. *Z. Anorg. Allg. Chem.* **1987**, *555*, 129.
(18) Garces, J. M.; Rocke, S. C.; Crowder, C. E.; Hasha, D. L. *Clays Clay Miner.* **1988**, *36*, 409.
(19) Almond, G. G.; Harris, R. K.; Graham, P. *J. Chem. Soc., Chem. Commun.* **1994**, 851.
(20) Almond, G. G.; Harris, R. K.; Franklin, K. R. *J. Mater. Chem.* **1997**, *7*, 681.
(21) Almond, G. G.; Harris, R. K.; Franklin, K. R.; Graham, P. *J. Mater. Chem.* **1996**, *6*, 843.
(22) Hanaya, M.; Harris, R. K. *J. Mater. Chem.* **1998**, *8*, 1073.
(23) Skibsted, J.; Bildsøe, H.; Jakobsen, H. J. *J. Magn. Reson.* **1991**, *92*, 669.
(24) Skibsted, J.; Nielsen, N. C.; Bildsøe, H.; Jakobsen, H. J. *J. Magn. Reson.* **1991**, *95*, 88.
(25) Skibsted, J.; Vosegaard, T.; Bildsøe, H.; Jakobsen, H. J. *J. Phys. Chem.* **1996**, *100*, 14872.

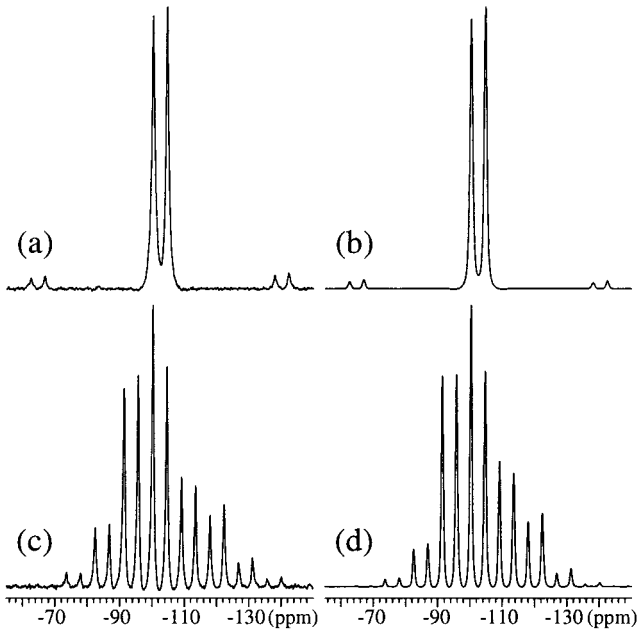

Figure 2. ^{29}Si{^{1}H} CP/MAS NMR spectra of searlesite recorded at spinning speeds of (a) $\nu_R = 3000$ Hz and (c) 700 Hz using a CP contact time of 5 ms, a 4-s repetition delay, and 512 scans. Simulated spectra of the manifolds of ssbs originating from the CSA interaction using the parameters listed in Table 1 are shown in parts (b) and (d).

Table 1. ^{29}Si Chemical Shift Parameters for the Two Silicon Sites in Searlesite[a]

	δ_σ (ppm)	η_σ	δ_{iso} (ppm)
Si(1)[b]	22.0 ± 1.6	0.54 ± 0.11	−100.3 ± 0.2
Si(2)[b]	24.5 ± 1.4	0.50 ± 0.10	−104.7 ± 0.2
	δ_{11} (ppm)	δ_{22} (ppm)	δ_{33} (ppm)
Si(1)	−83.4 ± 2.6	−95.3 ± 1.9	−122.3 ±1.8
Si(2)	−86.3 ± 2.5	−98.6 ± 1.8	−129.2 ± 1.6

[a] The CSA parameters (δ_σ and η_σ) are defined by the principal elements of the CSA tensors as $\delta_\sigma = \delta_{iso} - \delta_{33}$ and $\eta_\sigma = (\delta_{11} - \delta_{22})/\delta_\sigma$, where $\delta_{iso} = (\delta_{11} + \delta_{22} + \delta_{33})/3$ and the δ_{ii} elements fulfill the condition $|\delta_{33} - \delta_{iso}| \geq |\delta_{11} - \delta_{iso}| \geq |\delta_{22} - \delta_{iso}|$. δ_{iso} and the δ_{ii} elements are reported relative to tetramethylsilane (TMS). [b] Assignment of the ^{29}Si CSA parameters to the two silicon sites in searlesite using the same indexing as in the single-crystal X-ray diffraction structure[11] (see text).

the two silicon sites, as compared to those generally observed for $Si(OSi)_4$ species,[26] most likely reflect the presence of the $BO_2(OH)_2$ functionality in the first coordination sphere of each silicon as seen in Figure 1. A similar effect on the ^{29}Si CSA has been observed for the sodalite structure of the mineral tugtupite ($Na_8Al_2Be_2Si_8O_{24}Cl_2$, $\delta_\sigma = 48$ ppm and $\eta_\sigma = 0.57$),[27] in which each silicon tetrahedron is connected to two SiO_4 units, one AlO_4 and one BeO_4 tetrahedron. Although the δ_{iso} values for the two silicon sites in searlesite only differ by 4.4 ppm, an assignment of these resonances to the two distinct silicon sites is proposed on the basis of the correlation by Sherriff and Grundy[28] between δ_{iso}(^{29}Si) and the magnetic anisotropies and valences of the bonds between oxygen and the second-neighbor cations to silicon. Employing this approach and the structural data reported for searlesite[11] results in calculated isotropic chemical shifts of −97.1 and −99.1 ppm for Si(1) and Si(2), respectively. These values suggest that the observed chemical shifts of −100.3 and −104.7 ppm should be assigned to the Si(1) and Si(2) sites, respectively. The high-frequency shifts of 3−4 ppm for the calculated δ_{iso}(^{29}Si) values relative to the observed chemical shifts may possibly reflect hydrogen-bonding effects in the structure, although the oxygen atoms within the first coordination sphere of the silicon atoms are not themselves directly involved in hydrogen bonding. The same assignment of the δ_{iso} values given above is also obtained using the group electronegativity approach of Janes and Oldfield[29] when effects from the Si−O−Si/B angles on the group electronegativities are considered. An assignment of the two ^{29}Si resonances may also be obtained from the CP cross relaxation time constants, T_{CP}, determined from variable-contact time {^{1}H}^{29}Si CP/MAS NMR experiments, using the fact that T_{CP} is inversely proportional to the heteronuclear dipolar second moment $\langle M_2(SiH)\rangle$.[30] This relationship has recently been used to locate organic guest molecules in zeolites from {^{1}H}^{29}Si CP/MAS NMR spectra.[31] By employing the approach by Van Vleck,[32] the second moment can be calculated from the internuclear Si−H distances (r_{SiH}) using the equation

$$\langle M_2(SiH)\rangle = (1/5)(\gamma_H\gamma_{Si}\mu_0 h/16\pi^3)^2/\sum(r_{SiH})^6 \qquad (1)$$

where γ_H and γ_{Si} are the gyromagnetic ratios for ^{1}H and ^{29}Si, and the summation includes the H atoms in close proximity to the Si atoms. Using this equation for the H atoms within a 5 Å distance to the silicon atoms and the structural data from X-ray diffraction[11] gives the second moments $\langle M_2(SiH)\rangle = 1.86 \times 10^7$ Hz^2 and $\langle M_2(SiH)\rangle = 1.30 \times 10^7$ Hz^2 for the Si(1) and Si(2) sites, respectively. From {^{1}H}^{29}Si CP/MAS NMR experiments recorded with contact times in the range 0.05−50 ms, we obtain $T_{CP} = 1.87 \pm 0.06$ ms and $T_{CP} = 2.84 \pm 0.06$ ms for the ^{29}Si resonances at −100.3 and −104.7 ppm, respectively. These values result in the assignment of the resonances at −100.3 and −104.7 ppm to the Si(1) and Si(2) sites, respectively, in agreement with the assignment obtained above from the chemical shift−structure relationships.

The ^{1}H MAS NMR spectrum of searlesite (Figure 3) shows clearly resolved resonances from the two inequivalent hydrogen atoms with chemical shifts $\delta_{iso} = 4.4 \pm 0.1$ ppm and $\delta_{iso} = 2.2 \pm 0.1$ ppm. The observation of two ^{1}H resonances with relatively small line widths under MAS conditions indicates that there are only small ^{1}H−^{1}H dipolar couplings between the two sites consistent with their low concentrations and relative isolation in the structure due to the relative orientation of the two B−OH groups as seen in Figure 1 (i.e., the shortest ^{1}H−^{1}H distance is 3.14 Å).[11]

The ^{23}Na MAS NMR spectrum of searlesite (Figure 4a) shows a well-defined second-order quadrupolar line shape for the central ($m = {}^1/_2 \leftrightarrow m = -{}^1/_2$) transition, originating from the unique sodium site in the structure. Least-squares fitting to the quadrupolar line shape gives the ^{23}Na quadrupole coupling parameters and the isotropic chemical shift listed in Table 2 with the simulated spectrum shown in Figure 4b. The ^{11}B MAS NMR spectrum of searlesite (Figure 5a) shows a clearly defined manifold of ssbs from the satellite ($m = \pm {}^3/_2 \leftrightarrow m = \pm {}^1/_2$)

(26) Stebbins, J. F. In *Handbook of Physical Constants*; Arhrens, T., Ed.; American Geophysical Union: Washington, DC, 1995; Vol. 2, p 303.
(27) Skibsted, J.; Norby, P.; Bildsøe, H.; Jakobsen, H. J. *Solid State Nucl. Magn. Reson.* **1995**, *5*, 239.
(28) Sherriff, B. L.; Grundy, H. D. *Nature* **1988**, *332*, 819.
(29) Janes, N.; Oldfield, E. *J. Am. Chem. Soc.* **1985**, *107*, 6769.
(30) Pines, A.; Gibby, M. G.; Waugh, J. S. *J. Chem. Phys.* **1973**, *59*, 569.
(31) Fyfe, C. A.; Diaz, A. C.; Lewis, A. R.; Chézeau, J. M.; Grondey, H.; Kokotailo, G. T. In *Solid-State NMR Spectroscopy of Inorganic Materials*; Fitzgerald, J. J., Ed.; ACS Symposium Series 717; American Chemical Society: Washington, DC, 1999; p 283.
(32) Van Vleck, J. H. *Phys. Rev.* **1948**, *74*, 1168.

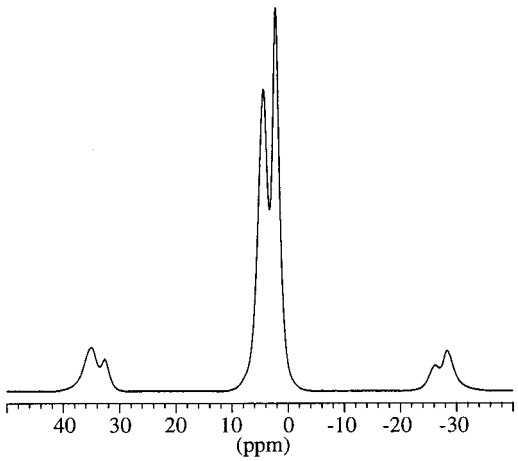

Figure 3. ^{1}H MAS NMR spectrum of searlesite recorded at a spinning speed of $\nu_R = 10.0$ kHz, using a repetition delay of 10 s and 80 scans.

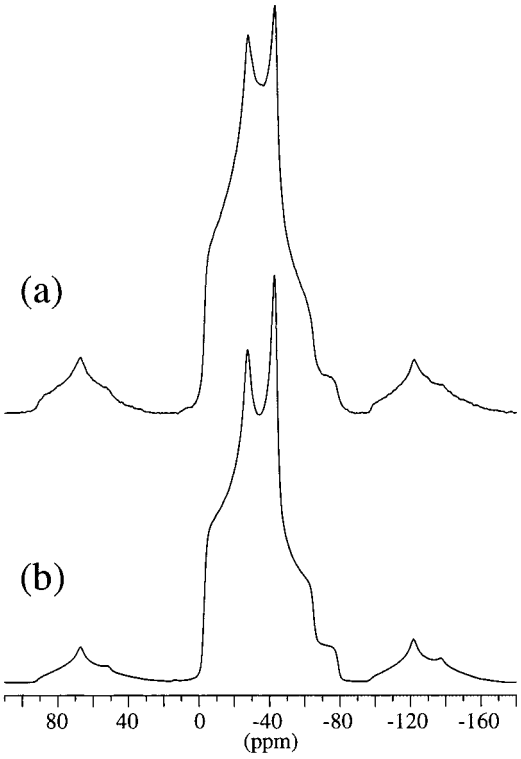

Figure 4. (a) ^{23}Na MAS NMR spectrum of the central transition for searlesite ($\nu_R = 10.0$ kHz). The simulated spectrum (b) results from least-squares fitting to the second-order quadrupolar line shape in (a) which gives the C_Q, η_Q, and δ_{iso} parameters listed in Table 2.

Table 2. ^{11}B and ^{23}Na Quadrupole Coupling Parameters and Isotropic Chemical Shifts for Searlesite

	C_Q (MHz)	η_Q	$\delta_{iso}{}^a$ (ppm)
^{11}B	0.501 ± 0.010	0.99 ± 0.03	42.4 ± 0.3
^{23}Na	3.64 ± 0.03	0.58 ± 0.02	−1.4 ± 0.3

[a] The ^{11}B and ^{23}Na isotropic chemical shifts are relative to a solid sample of $NaBH_4$ and to a 1.0 M aqueous solution of NaCl, respectively.

transitions for the unique boron site in the structure. Least-squares optimization to the intensities of the ssbs in the manifold yields the ^{11}B quadrupole coupling parameters and the isotropic chemical shift listed in Table 2 with the simulated spectrum in Figure 5b. The relatively small quadrupole coupling constant

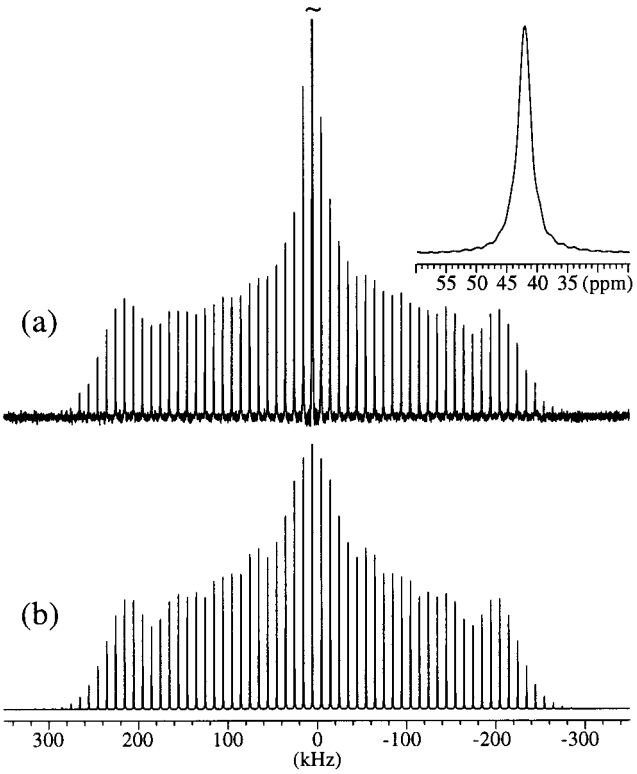

Figure 5. (a) ^{11}B MAS NMR spectrum of the central and satellite transitions for searlesite obtained at a spinning speed of $\nu_R = 10.0$ kHz with a 0.5 s repetiton delay and 4096 scans. The inset in (a) illustrates the centerband from the central transition on a normalized intensity scale. (b) Simulated spectrum of the satellite transitions in (a) using the C_Q, η_Q, and δ_{iso} parameters listed in Table 2 for searlesite.

of $C_Q = 0.501$ MHz is a characteristic feature for tetrahedral BO_4 species.[33,34] Larger ^{11}B quadrupole couplings (i.e., $C_Q = 2.5$ MHz) are generally observed for trigonal boron sites (BO_3 units) such as those found in glasses.[33,34]

Thus, the NMR data determined for ^{1}H, ^{11}B, ^{23}Na, and ^{29}Si are all consistent with the numbers and types of local environments obtained from the X-ray diffraction-determined crystal structure, and they demonstrate that the synthetic sample of searlesite studied in the present work is crystalline with a high degree of both short- and long-range order. Furthermore, the very asymmetric (but very well-defined) local environments of the silicon, sodium, and boron sites mean that the parameters characterizing the anisotropic NMR interactions (Tables 1 and 2) provide a unique fingerprinting of the structure. Thus, these parameters are diagnostic of the whole framework structure and can be used to identify searlesite, even in complex mixtures and in situations where its occurrence is not anticipated.

Product Mixtures. The product mixtures described in this section were produced in an attempt to incorporate boron atoms into the layer silicates magadiite and kenyaite by conducting the syntheses in the presence of a source of boron as described in the Experimental Section. Preliminary investigations indicated additional signals in the ^{29}Si MAS NMR spectra and additional reflections in the powder XRD patterns, suggesting possible structural modifications for both layer silicates. However, as described below, a more detailed study clearly indicated the (unexpected) presence of searlesite and the formation of mixtures from both of these syntheses.

(33) Bray, P. J. *J. Non-Cryst. Solids* **1985**, *75*, 29.
(34) Turner, G. L.; Smith, K. A.; Kirkpatrick, R. J.; Oldfield, E. *J. Magn. Reson.* **1986**, *67*, 544.

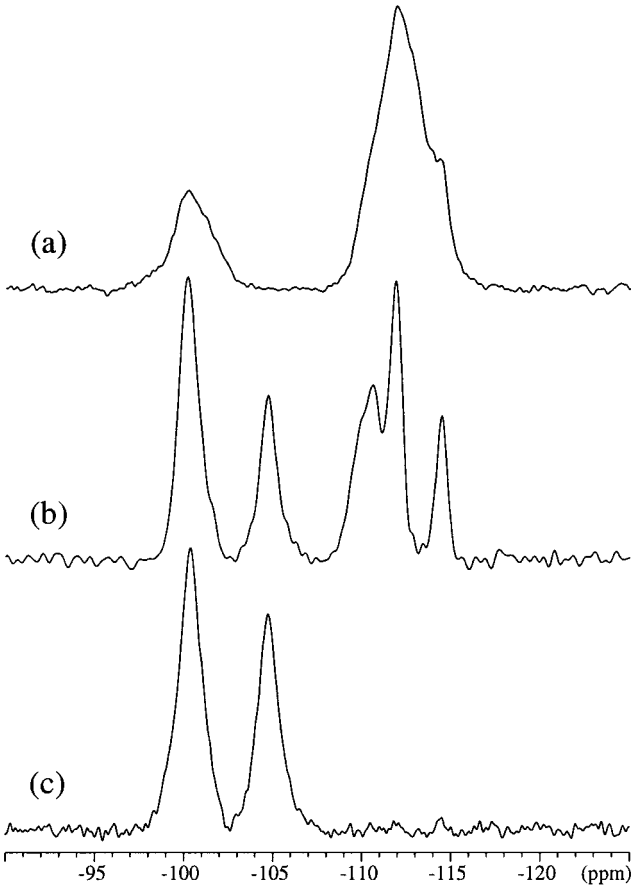

Figure 6. ^{29}Si MAS NMR spectra ($\nu_R = 3.0$ kHz) of synthetic samples of (a) sodium magadiite (500-s repetition delay, 88 scans) and (b) magadiite produced from a boron-containing medium (2000-s repetition delay, 32 scans). (c) ^{29}Si{^{1}H} CP/MAS spectrum ($\nu_R = 2.6$ kHz) of the same sample as in (b) obtained using a CP contact time of 5 ms, a 4-s repetition delay, and 256 scans.

Figure 6a shows the ^{29}Si MAS NMR spectrum of a typical sample of synthetic sodium magadiite ($Na_2Si_{14}O_{30}\cdot xH_2O$, $x = 8-10$), where the ^{29}Si resonances at approximately -100 ppm originate from HOSi*$(OSi)_3$ or NaOSi*$(OSi)_3$ sites (i.e., Q^3 units), while the partly resolved peaks from -109 to -115 ppm are assigned to Si*$(OSi)_4$ species (Q^4 units). This interpretation is in full agreement with earlier ^{29}Si MAS NMR investigations of natural and synthetic magadiite samples.[12-20] Furthermore, the observed Q^3:Q^4 of 1:2.95 (± 0.1) for the spectrum in Figure 6a is in good agreement with the ratio Q^3:Q^4 of 1:3 reported for a mineral sample of magadiite,[14] indicating that the ^{29}Si MAS NMR spectrum (Figure 6a) was collected under conditions that allow full ^{29}Si spin$-$lattice relaxation. The ^{29}Si MAS NMR spectrum of the product from the boron-containing reaction mixture (Figure 6b) shows that the resonances from the latter material exhibit much smaller line widths compared to those observed for the magadiite sample from a conventional synthesis (Figure 6a) which indicates a much higher degree of local ordering and hence crystallinity. Furthermore, there is also the appearance of an additional resonance at -104 ppm which could possibly be due to silicon atoms connected to boron. However, a {^{1}H}^{29}Si CP/MAS NMR experiment on this sample (Figure 6c) clearly shows the characteristic ^{29}Si spectral pattern for searlesite as described in detail above (cf. Figure 2). Furthermore, the approximately 1:1 intensity ratio for the two resonances in the {^{1}H}^{29}Si CP/MAS NMR spectrum (Figure 6c) indicates that CP is much more efficient for the silicon sites in searlesite compared to the HOSi*$(OSi)_3$ sites in magadiite, and that this technique is a useful tool to distinguish these phases in mixtures. Thus, the ^{29}Si NMR spectra in Figure 6b and c demonstrate that the material from the boron-containing synthesis is a mixture of searlesite and magadiite. This is further confirmed by the ^{11}B and ^{23}Na MAS NMR spectra of the same material shown in Figure 7a and b, respectively. The ^{11}B MAS spectrum displays a single resonance from the central transition with a line width of fwhm $= 2.4$ ppm and a center of gravity at $\delta_{cg} = 41.9$ ppm in full agreement with the spectrum of searlesite described above. Furthermore, the observation of only a single resonance with a small line width indicates that boron has not been incorporated into the magadiite phase. The ^{23}Na MAS spectrum of the material from the boron-containing synthesis (Figure 7b) is composed of two centerbands corresponding to the sodium sites in sodium magadiite (Figure 7d) and searlesite (Figure 7e). Since a very small pulse angle was used, the intensities are independent of the quadrupolar couplings, and this spectrum can be used to directly determine the proportions of the two components. Deconvolution of the spectrum in Figure 7b, employing the quadrupole coupling parameters and δ_{iso} values for searlesite in Table 2 and those reported for a synthetic sample of sodium magadiite,[22] gives the simulated spectrum in Figure 7c which corresponds to the ^{23}Na intensity ratio of 1.0:2.5 for magadiite and searlesite. Assuming the composition of $Na_2Si_{14}O_{29}\cdot 8H_2O$ for sodium magadiite, as earlier reported from the chemical analysis of a mineral sample,[35] the molar intensity ratio corresponds to a composition of 51 wt % sodium magadiite and of 49 wt % searlesite for the material from a boron-containing synthesis.

Similar results are observed for the kenyaite sample obtained from the boron-containing synthesis (see Experimental Section), in that the ^{11}B, ^{23}Na, and ^{29}Si MAS NMR spectra clearly reveal that the product from this synthesis is a mixture of kenyaite and searlesite. The ^{29}Si MAS NMR spectrum of the synthesis product is shown in Figure 8a which in addition to the peaks originating mainly from searlesite (Figure 8b) includes at least six resonances at $\delta_{iso} = -108.5$, -110.8, -111.5, -113.2, -113.7, and -118.9 ppm which are assigned to Q^4 sites in kenyaite. Furthermore, we expect that a resonance about -100 ppm from a Q^3 site in kenyaite also contributes with intensity to the resonance at -100.3 ppm. The ^{11}B MAS spectrum (not shown) confirms the presence of searlesite and indicates that boron has not been incorporated in the kenyaite structure. The ^{23}Na MAS spectrum (not shown) displays two centerbands originating from sodium in kenyaite and searlesite. As previously, the intensities of the two components are independent of the quadrupolar couplings and can be used to determine their proportions in the mixture. Deconvolution of this spectrum gives the intensity ratio of 1:4.2 for Na in kenyaite and searlesite which corresponds to the composition of 46 wt % kenyaite and of 54 wt % searlesite, assuming the kenyaite has the oxide formula $Na_2Si_{20}O_{41}\cdot 10H_2O$.

With the information from the NMR investigations that searlesite-containing mixtures are produced, it is now possible to correctly interpret the associated changes in their powder XRD patterns as shown in Figure 9. Compared to the pattern of synthetic sodium magadiite (Figure 9a), that of the magadiite material from the boron-containing synthesis (Figure 9b) shows additional reflections with the lowest one at an angle of 11° 2Θ. As mentioned, these were thought to possibly indicate that boron sites "bridged" between specific sites on different layers were formed, resulting in a different and more highly ordered

(35) Gude, A. J.; Sheppard, R. A. *Am. Mineral.* **1972**, *57*, 1053.

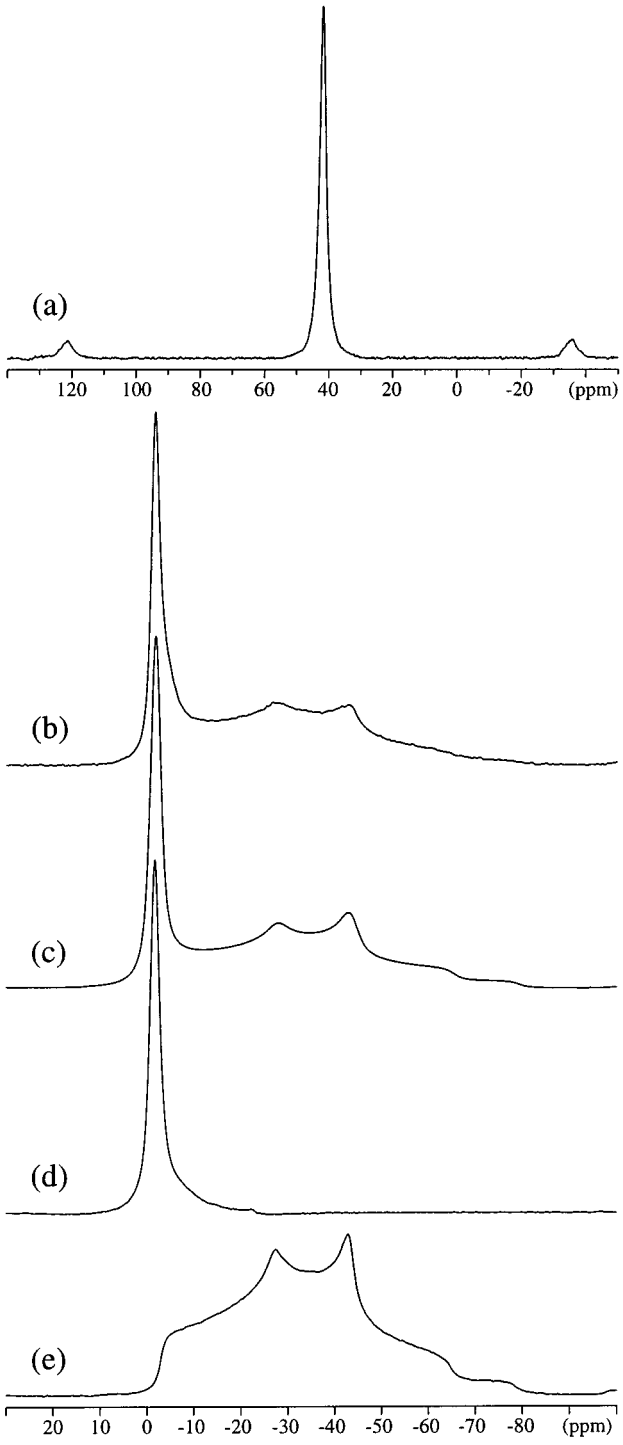

Figure 7. (a) ^{11}B MAS NMR spectrum of the central transition for the magadiite sample from the boron-containing synthesis mixture (ν_R = 10.0 kHz, 1-s repetition delay, and 1456 scans). (b) ^{23}Na MAS NMR spectrum of the central transitions for the same material. The experimental spectrum was obtained using ν_R = 10.0 kHz, a 2-s repetition delay, and 512 scans. (c) Simulation of the spectrum in part (b) using two second-order quadrupolar line shapes corresponding to the C_Q, η_Q, and δ_{iso} parameters reported for sodium magadiite (δ_{iso} = −0.9 ppm, $C_Q(1 + \eta_Q^2/3)^{1/2}$ = 0.61 MHz)[22] and searlesite (see Table 2). The simulation employed an intensity ratio of 1.0:2.5 for sodium in magadiite and searlesite, respectively. Experimental ^{23}Na MAS NMR spectra (ν_R = 10.0 kHz and a 2-s repetition delay) of a synthetic sodium magadiite (512 scans) and searlesite (2048 scans) are shown in parts (d) and (e), respectively, and serve to illustrate that the spectrum of magadiite from the boron-contaning synthesis in part (b) includes central transitions from these two phases.

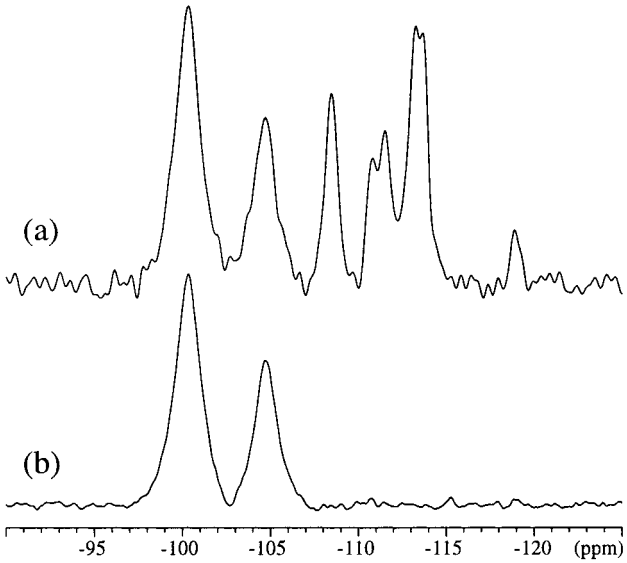

Figure 8. (a) ^{29}Si MAS NMR spectrum of the synthetic sample of kenyaite produced from a boron-containing medium (ν_R = 3.3 kHz, a 500-s repetition delay, and 30 scans). (b) ^{29}Si{^{1}H} CP/MAS spectrum of the same sample as in (a) obtained using ν_R = 2.7 kHz, a CP contact time of 2 ms, a 4-s repetition delay, and 256 scans.

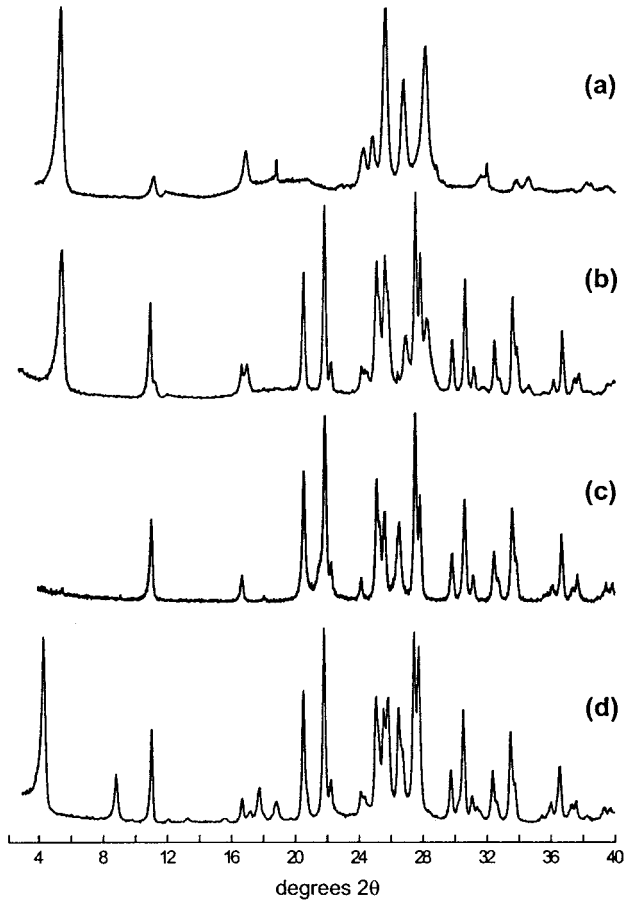

Figure 9. Powder XRD patterns for the synthetic samples of (a) sodium magadiite, (b) magadiite produced from a boron-containing medium, (c) searlesite, and (d) kenyaite produced from a boron-containing synthesis medium.

structure. However, from the information provided by the NMR experiments, these reflections and those in the corresponding pattern of the kenyaite material (Figure 9d) are readily identified as arising from the searlesite component of the mixture. The

XRD pattern for searlesite is shown in Figure 9c, and a comparison of this diagram with those observed for the magadiite and kenyaite samples produced from the boron-containing syntheses (Figure 9b and d) clearly reveals that the searlesite component accounts for most of the reflections in these diagrams at high 2Θ angles.

Conclusions

The solid-state MAS NMR spectra of ^{1}H, ^{11}B, ^{23}Na, and ^{29}Si in searlesite and the anisotropic NMR parameters determined from these spectra reflect the local environments of the X-ray-determined structure and when used together provide a unique diagnostic probe for this structure. Similar experiments on the materials produced from the syntheses of magadiite and kenyaite in boron-containing media show that they are, in fact, mixtures containing searlesite. It is anticipated that studies of this type will provide similar information in a variety of other situations and should be considered when investigating products from boron-containing synthesis mixtures.

The results indicate that searlesite formation consumes all of the boron in these synthesis mixtures. However, the presence of boron in the mixture does appear to have an important influence on the quality of the magadiite- and kenyaite-layered silicates produced. The structures of these materials are still unknown, and the samples present in the mixtures are much more highly ordered than the synthetic materials previously produced in terms of both long-range periodicity (XRD) and short-range ordering (NMR). If the components of the mixtures could be separated, structural investigations of powder XRD data using direct methods techniques may be possible.

Acknowledgment. We acknowledge the financial assistance of the NSERC of Canada in the form of operating and equipment grants (C.A.F.). J.S. thanks the Danish Natural Science Research Council (J. No. 9600396 and 0001237) for financial support. W.S. acknowledges the Alexander von Humbolt Foundation and the German Research Foundation, DFG (Projects Schw 478/1 and 478/5) for financial support. Dr. Andrew R. Lewis (University of British Columbia) is acknowledged for his assistance in the preparation of this manuscript.

IC010487S